

University of Massachusetts Medical School
eScholarship@UMMS

GSBS Student Publications

Graduate School of Biomedical Sciences

2011-08-01


A novel zinc binding system, ZevAB, is critical for survival of nontypeable *Haemophilus influenzae* in a murine lung infection model

Charles V. Rosadini
University of Massachusetts Medical School

Et al.

Let us know how access to this document benefits you.

Follow this and additional works at: https://escholarship.umassmed.edu/gsbs_sp

 Part of the [Medicine and Health Sciences Commons](#), [Microbiology Commons](#), and the [Physiology Commons](#)

Repository Citation

Rosadini CV, Gawronski JD, Raimunda D, Argüello J, Akerley BJ. (2011). A novel zinc binding system, ZevAB, is critical for survival of nontypeable *Haemophilus influenzae* in a murine lung infection model. GSBS Student Publications. <https://doi.org/10.1128/IAI.05135-11>. Retrieved from https://escholarship.umassmed.edu/gsbs_sp/1774

This material is brought to you by eScholarship@UMMS. It has been accepted for inclusion in GSBS Student Publications by an authorized administrator of eScholarship@UMMS. For more information, please contact Lisa.Palmer@umassmed.edu.

A Novel Zinc Binding System, ZevAB, Is Critical for Survival of Nontypeable Haemophilus influenzae in a Murine Lung Infection Model

Charles V. Rosadini, Jeffrey D. Gawronski, Daniel
Raimunda, José M. Argüello and Brian J. Akerley
Infect. Immun. 2011, 79(8):3366. DOI: 10.1128/IAI.05135-11.
Published Ahead of Print 16 May 2011.

Updated information and services can be found at:
<http://iai.asm.org/content/79/8/3366>

SUPPLEMENTAL MATERIAL

These include:

<http://iai.asm.org/content/suppl/2011/07/08/79.8.3366.DC1.html>

REFERENCES

This article cites 73 articles, 36 of which can be accessed free
at: <http://iai.asm.org/content/79/8/3366#ref-list-1>

CONTENT ALERTS

Receive: RSS Feeds, eTOCs, free email alerts (when new
articles cite this article), [more»](#)

Information about commercial reprint orders: <http://iai.asm.org/site/misc/reprints.xhtml>
To subscribe to to another ASM Journal go to: <http://journals.asm.org/site/subscriptions/>

A Novel Zinc Binding System, ZevAB, Is Critical for Survival of Nontypeable *Haemophilus influenzae* in a Murine Lung Infection Model^{∇†}

Charles V. Rosadini,¹ Jeffrey D. Gawronski,¹ Daniel Raimunda,²
José M. Argüello,² and Brian J. Akerley^{1*}

Department of Microbiology and Physiological Systems, University of Massachusetts Medical School, Worcester, Massachusetts 01655,¹
and Department of Chemistry and Biochemistry, Worcester Polytechnic Institute, Worcester, Massachusetts 01609²

Received 25 March 2011/Returned for modification 17 April 2011/Accepted 8 May 2011

Nontypeable *Haemophilus influenzae* (NTHI) is a Gram-negative bacterial pathogen that causes upper and lower respiratory infections. Factors required for pulmonary infection by NTHI are not well understood. Previously, using high-throughput insertion tracking by deep sequencing (HITS), putative lung colonization factors were identified. Also, previous research indicates that secreted disulfide-dependent factors are important for virulence of *H. influenzae*. In the present study, HITS data were compared with an informatics-based list of putative substrates of the periplasmic oxidoreductase DsbA to find and characterize secreted virulence factors. This analysis resulted in identification of the “zinc binding essential for virulence” (*zev*) locus consisting of *zevA* (HI1249) and *zevB* (HI1248). NTHI mutants of *zevA* and *zevB* grew normally in rich medium but were defective for colonization in a mouse lung model. Mutants also exhibited severe growth defects in medium containing EDTA and were rescued by supplementation with zinc. Additionally, purified recombinant ZevA was found to bind to zinc with high affinity. Together, these data demonstrate that *zevAB* is a novel virulence factor important for zinc utilization of *H. influenzae* under conditions where zinc is limiting. Furthermore, evidence presented here suggests that zinc limitation is likely an important mechanism for host defense against pathogens during lung infection.

Nontypeable *Haemophilus influenzae* (NTHI) is a Gram-negative bacterial pathogen uniquely adapted to colonize the nasopharynx of healthy humans, with a carriage frequency of approximately 20 to 80% (46). An opportunistic pathogen, NTHI resides asymptotically in the upper airways of humans but can disseminate into privileged anatomical locations, causing infections such as otitis media, sinusitis, and pneumonia (47). NTHI is also one of the most prevalent microorganisms found in the lungs of patients with exacerbations of chronic obstructive pulmonary disease (48, 49, 60) and cystic fibrosis (23, 43, 58). An effective vaccine against NTHI strains has not yet been discovered, likely due to high variability of surface antigens between strains (60).

Little is known regarding factors required for survival of *H. influenzae* in the lung. To address this, we recently examined a transposon mutant library of *H. influenzae* Rd in a mouse lung infection model using a novel technique termed high-throughput insertion tracking by deep sequencing (HITS) (22). HITS analysis revealed a total of 136 genes required for survival in this site, including previously identified virulence determinants, such as those involved in lipooligosaccharide synthesis (51), as well as several genes previously unrecognized to play a role in pathogenesis, some of which are implicated in diverse

processes, including DNA repair, membrane remodeling, and nutrient acquisition. However, many genes identified by HITS have unknown functions and have yet to be characterized.

Previously, the periplasmic disulfide bond pathway was investigated to find virulence determinates of *H. influenzae* (56). Disulfide formation is mediated by the periplasmic oxidoreductase protein DsbA, which directly catalyzes disulfide bond formation by transferring its disulfide to free thiol groups of cysteine residues in secreted target proteins (19, 76). This system is important for providing structural stability and function to secreted virulence factors in a range of bacterial pathogens (30). DsbA was demonstrated to be required for pathogenesis of *H. influenzae* in a mouse model of bacteremia (56). Additionally, the heme-binding lipoprotein HbpA, an important factor required for growth of *H. influenzae* on several heme sources (26, 44), was found to be a substrate of DsbA and was required for pathogenesis. However, the defect of an *hbpA* mutant was not as severe as that of a *dsbA* mutant, suggesting that other, unidentified DsbA-dependent factors must be required for pathogenesis.

Since a DsbA-dependent protein was found to have a role in virulence of *H. influenzae*, we hypothesized that by examining genes required in the lung, additional DsbA-dependent factors involved in infection could be found. In this study, potential DsbA substrates were identified based on predicted extracytoplasmic localization and putative disulfide bond formation. The whole-genome fitness data generated via the HITS procedure was used to identify candidate DsbA substrates required for survival of *H. influenzae* in the lung. This approach led us to characterize a locus important for zinc utilization, herein referred to as “zinc binding essential for virulence”

* Corresponding author. Mailing address: Department of Microbiology and Physiological Systems, University of Massachusetts Medical School, 55 Lake Ave. N., S6-242, Worcester, MA 01655. Phone: (508) 856-1442. Fax: (508) 856-1422. E-mail: Brian.Akerley@umassmed.edu.

† Supplemental material for this article may be found at <http://iai.asm.org/>.

∇ Published ahead of print on 16 May 2011.

(*zev*). This locus contains an operon consisting of two genes, the potential DsbA substrate *zevA* and a gene encoding a putative membrane protein called *zevB*. In contrast to the previously characterized ZnuABC zinc transport system, which is required for optimal growth in rich culture medium *in vitro* (39), the *zevAB* system is specifically required for growth under severe zinc limitation. The results of this study suggest that the lung represents a niche that exposes infecting pathogens to severe zinc limitation and that the *zevAB* system is required for zinc homeostasis of *H. influenzae* during pathogenesis.

MATERIALS AND METHODS

Strains and culture conditions. *H. influenzae* RdAW (GenBank accession no. NZ_ACSM00000000), a capsule-deficient serotype d derivative (70), and pathogenic nontypeable *H. influenzae* strain NT127 (GenBank accession no. NZ_ACSL00000000) were grown in brain heart infusion (BHI) broth supplemented with 10 µg/ml hemin and 10 µg/ml NAD (sBHI) or on sBHI agar plates at 35°C. To generate an anaerobic environment, strains were grown in anaerobic chambers with BBL GasPak Plus generators (Becton Dickinson and Company, Sparks, MD). Development of competence for transformation of *H. influenzae* was accomplished as previously described (5). For selection of Rd- and NTHI-derived strains, antibiotics were used at the following concentrations: 8 µg/ml tetracycline (Tc), 20 µg/ml kanamycin (Km), and 10 µg/ml gentamicin (Gm). For strain generation, plasmids and PCR products were constructed using standard molecular biology techniques (4). For complementation of mutants, DNA fragments were amplified by PCR and cloned between adjacent SapI restriction sites of the chromosomal delivery vector pXT10, linearized, and used to transform *H. influenzae* strains as previously described (70).

***zevA* strain construction.** The NTHI *zevA* mutant strain NT1249G was constructed by replacement of the coding sequence of *zevA* (NT127 locus tag HIAG_01363) with the Gm resistance cassette *aacCI*. To do this, a 707-bp PCR product containing the 5' flanking region of *zevA*, generated using primers 1249for and 1249B (see Table S1 in the supplemental material), a 762-bp PCR product containing the coding region for the Gm resistance cassette, generated with primers 5pGent1 and 3Gent2, and a 1,661-bp PCR product containing the 3' flanking region of *zevA*, generated with primers 1249A and 1248rev, were joined by overlap extension PCR, via complementary ends, using primers 1249for and 1248rev. The resulting 3,086-bp fragment was introduced into competent cells of strain NTX, a derivative of NT127 in which the xylose locus was modified for efficient recombination with plasmid pXT10 and its derivatives (28). Gm-resistant (Gm^r) transformants were selected on sBHI containing Gm, creating strain NTzevAG. NTzevAG was transformed with linearized "empty vector" pXT10, and Tc^r transformants were isolated to create strain NTzevAV. Double crossovers into the *zevA* locus were verified using primers 51249test and 31249test, which bind outside the recombination junctions.

To complement the *zevA* deletion, *zevA* and upstream promoter elements were amplified by PCR with primers 51249HA and 31249R, which introduce SapI restriction sites at the termini of the fragment. The resulting 1,017-bp fragment was digested with SapI and cloned into SapI-digested vector pXT10, creating plasmid pX1249J. Plasmid pX1249J was linearized with ApaLI and introduced into competent cells of strain NT1249G. Tc^r recombinants were selected on sBHI containing Tc, resulting in strain NTzevAX.

***zevB* strain construction.** Deletion of *zevB* in NTHI was also performed by replacement of the coding region of *zevB* (HIAG_01364) with the Gm resistance gene. To increase the efficiency of mutant selection, the *aacCI* promoter was replaced with the *H. influenzae* *arcA* promoter. First, a 1,332-bp fragment containing the 5' flanking region of *zevB*, amplified by PCR using NT127 genomic DNA as a template with primers 1249for and 1248JBpArcA, a 762-bp fragment carrying the *arcA* promoter fused to the coding region of the Gm resistance gene from *aacCI*, amplified from a pXT10 plasmid using primers 5pArcA and 3Gent2, and a 1,326-bp fragment containing the 3' flanking region of *zevB*, amplified from NT127 genomic DNA using primers 1248AHib and 1247RevJB, were joined by overlap extension PCR using primers 1249for and 1247RevJB. The resulting 3,638-bp fragment was used to transform competent cells of strain NTX. Gm^r transformants were selected on sBHI-Gm plates, resulting in strain NTzevBG. NTzevBG was then transformed with linearized vector pXT10, and Tc^r transformants were isolated to create strain NTzevBV. Double crossovers into the *zevB* locus were verified using primers 51249test and 31249test, which bind outside the recombination junctions.

To complement the *zevB* mutant, the region consisting of *zevA*, *zevB*, and

upstream promoter elements was amplified by PCR with primers 51249HA and 31248R, which introduce SapI restriction sites at the termini of the fragment. The resulting 1,988-bp fragment was digested with SapI and cloned into SapI-digested vector pXT10, creating plasmid pX1248J. Plasmid pX1248J was linearized with ApaLI and introduced into competent cells of strain NT1248G. Tc^r recombinants were selected on sBHI containing Tc, resulting in strain NTzevBX.

For performing mixed infections with *zevA* and *zevB* mutant strains, a reference strain featuring a xylose-inducible *lacZ* gene was generated by transforming NT127 with ApaLI-digested plasmid pXELacZ2, which contains *lacZ* in place of *xyIA*. Tc^r recombinants were selected on sBHI containing Tc, resulting in strain NTlacZ.

***znuA* and *znuBC* strain construction.** For generating an NTHI *znuA* (HIAG_01677) mutant, a 971-bp fragment containing the 5' flanking region of *znuA* was amplified from NT127 genomic DNA with primers 5ZnuA1 and 3ZnuA1. A 1,065-bp fragment containing the *trc* promoter fused to the Km resistance gene (*aphI*), amplified from plasmid pENTtrcK (containing the *mini-mariner* transposon *mmTrcK* previously described [22]) with primers IFTrcF and 3kan1, and a 1,065 bp fragment containing the 3' flanking region of *znuA*, amplified from NT127 genomic DNA with primers 5ZnuA3 and 3ZnuA3, were joined using overlap extension PCR by virtue of their complementary ends with primers 5ZnuA1 and 3ZnuA3. The resulting 3,033-bp fragment was introduced into competent cells of strains NTV, NTzevAV, and NTzevBV, and Km-resistant (Km^r) colonies were selected on sBHI-Km, resulting in strains NTznuA, NTzevAznuA, and NTzevBznuA, respectively. Double crossovers into the *znuA* locus were verified using primers 5znuAtest and 3znuAtest, which bind outside the recombination junctions.

For generating an NTHI *znuBC* (HIAG_00759 and HIAG_00758) mutant, a 1,592-bp fragment containing the 5' flanking region of the *znuBC* operon, amplified from NT127 genomic DNA with primers 5ZnuB1 and 3ZnuB1, the 1,065-bp fragment described above, containing the *trc* promoter fused to the Km resistance gene, and a 1,027 bp fragment containing the 3' flanking region of *znuBC*, amplified from NT127 genomic DNA with primers 5ZnuA3 and 3ZnuA3, were joined using overlap extension PCR by virtue of their complementary ends using primers 5ZnuB1 and 3ZnuB3. The resulting 3,700-bp fragment was introduced into competent cells of strains NTV, NTzevAV, and NTzevBV, and Km^r colonies were selected on sBHI-Km, resulting in strains NTznuBC, NTzevAznuBC, and NTzevBznuBC, respectively. Double crossovers into the *znuBC* locus were verified using primers 5znuBCtest and 3znuBCtest, which bind outside the recombination junctions.

***zevA* reporter strain construction.** To generate the reporter strain R5, we replaced the coding region of *zevAB* (HI1249 and HI1248) in Rd with a reporter construct containing the *lacZ* gene, designed to fuse the *zevA* promoter to the translational start of *lacZ*, and used the *tetAR* Tc resistance operon as a selectable marker. To do this, a 683-bp fragment containing the 5' flanking region from *zevA*, amplified by PCR from Rd genomic DNA with primers 1249for and 1249BL, a 6,869-bp fragment containing the *lacZ* gene and *tetAR*, amplified from plasmid pXELacZ2 with primers LacFor2 and tetB, and a 689-bp fragment containing the 3' flanking region of *zevB*, amplified from Rd genomic DNA with primers 1248AL and 1248rev, were joined using overlap extension PCR with primers 1249for and 1248rev. The resulting 8,188-bp fragment was used to transform Rd competent cells. Tc^r transformants were selected on medium containing Tc, resulting in strain R5.

To complement mutation of *zevAB* in R5, a 1,988-bp fragment containing the *zevAB* coding regions as well as upstream promoter elements was amplified by PCR from Rd genomic DNA with primers 51249HA and 31248R, which introduce SapI restriction sites at the termini. The resulting fragment was digested with SapI and cloned into SapI-digested vector pXT10, creating plasmid pX1248R. Next, a 2,891-bp fragment containing the *xyIF* gene as well as the 5' flanking and coding regions of *zevAB*, amplified from plasmid pX1248R with primers pXT10thyAF and 31248gent, the 762-bp Gm resistance cassette fragment described above, and a 1,794-bp fragment containing the *xyIB* gene, amplified from pXT10 with primers 5xyIBgent and 3revrfad1, were joined using overlap extension PCR with primers pXT10thyAF and 3revrfad1. The resulting 5,447-bp fragment was used to transform competent cells of strain R5, resulting in R5X.

***fnr* mutant construction.** For mutation of *fnr* (HI1425), a 4,230-bp fragment containing the *fnr* gene with a *magellan1* transposon insertion ~170 bp from the 5' end of the FNR translational start was amplified by PCR from previously described strain Rfnr (28) with primers 5FNRcloning and 3FNRcloning and used to transform competent R5 cells. Km^r transformants were selected on sBHI-Km, and the mutation was verified by PCR, resulting in strain R5fnr.

To complement the *fnr* mutation, a 2,201-bp fragment containing *xyIF*, the *fnr* promoter, and *fnr* (amplified by PCR from strain RfnrC with primers pxt10thyAF

and 3FNRgent), the 762-bp Gm resistance cassette fragment described above, and a 1,794-bp fragment containing the *xyfB* gene (amplified from pXT10 with primers 5xyfBgent and 3revrfad1) were joined using overlap extension PCR with primers pXT10thyAF and 3revrfad1. The resulting 4,733-bp fragment was used to transform competent cells of strain R5fnr, and the mutation was verified by PCR, resulting in strain R5fnrX.

His-tagged ZevA construction. To generate the ZevA-His fusion, a 618-bp fragment containing the *zevA* gene was amplified from NT127 genomic DNA template with primers 51249JTOPO and 31249JTOPO. Primer 31249JTOPO adds a tobacco etch virus (TEV) protease cleavage site to the 3' end of the *zevA* gene (66). The 618-bp fragment was then TA cloned into the pBAD-TOPO-TA cloning vector (Invitrogen, Carlsbad, CA), which adds a C-terminal 6×His tag (immediately after the TEV cleavage site), and transformed into One Shot TOP10 *E. coli* (Invitrogen, Carlsbad, CA), creating strain ECZevAHIS, which harbors plasmid pZevAHIS. Plasmid pZevAHIS was verified by sequencing.

Genetic footprinting. *H. influenzae* Rd genomic DNA from input and output libraries was used as a template for genetic footprinting analysis as previously described (1, 61). PCRs were performed using the transposon-specific primer marout and gene-specific primer 3129rev, which binds 661 bp downstream of the *zevB* gene, and visualized on a 0.9% agarose gel stained with ethidium bromide. Migration distances and gene positions were determined as described previously (22, 59).

Murine lung infection model. Standing overnight cultures were used to inoculate 25 ml of sBHI in a 50-ml flask to a final optical density at 600 nm (OD_{600}) of 0.01. The resulting cultures were incubated with shaking at 250 rpm and 35°C until mid-log phase. Experimental strains were either mixed with the NTlacZ reference strain at a 1:1 ratio (mixed infections) or not mixed (single-strain infections), washed, and diluted in Hanks balanced salt solution (HBSS) to obtain a final concentration of 5×10^8 bacteria per ml. Forty microliters of bacteria (2×10^7 CFU total) was inoculated into the nares of female 6.5-week-old C57BL/6 mice (Charles River Laboratories, Boston, MA) anesthetized with ketamine (65 mg/kg of body weight) and xylazine (6.5 mg/kg) by intraperitoneal (i.p.) injection. At 40 h of infection, lungs were harvested and homogenized using a Fisher Tissuemiser homogenizer. Dilutions of the lung homogenate were plated on sBHI agar plates with or without 1 mM D-xylose and X-Gal (5-bromo-4-chloro-3-indolyl β -D-galactopyranoside; Sigma-Aldrich, St. Louis, MO) for CFU enumeration. For statistical analysis of mixed infections, the ratio of each experimental strain to NTlacZ was calculated, multiplied by 100, \log_{10} transformed, and analyzed using one-way analysis of variance (ANOVA) with Tukey's multiple-comparison test (Prism 5.03; GraphPad Software, La Jolla, CA). For single-strain infections, numbers of CFU per lung were calculated and analyzed by *t* test. All animal procedures were conducted in accordance with NIH guidelines and with prior approval by the University of Massachusetts Medical School Institutional Animal Care and Use Committee.

EDTA sensitivity and growth curve analysis. Strains were inoculated from standing overnight cultures at an OD_{600} of 0.01 into 25 ml of sBHI in a 50-ml flask and incubated with shaking at 250 rpm and 35°C until mid-log phase. These cultures were used to inoculate sBHI medium containing EDTA (at the final concentrations specified) at an OD_{600} of 0.02, and 100 μ l was dispensed into the wells of a 96-well microtiter plate (Corning) pre-filled with 100 μ l sBHI broth containing EDTA (final concentrations specified in Results). When necessary, the medium was supplemented with $MgCl_2$, $CaCl_2$, $MnCl_2$, $FeCl_3$, $CoCl_2$, $NiCl_2$, $CuSO_4$, $ZnSO_4$, or Na_2MoO_4 to a final concentration of 30 or 60 μ M. As a control, strains were also grown in sBHI medium without additions. For double mutant analysis, strains were grown in medium containing various concentrations of EDTA (final concentration of 0.0025 mM, 0.005 mM, or 0.01 mM) or medium containing various concentrations of $ZnSO_4$ (final concentration of 0.001 mM, 0.003 mM, or 0.05 mM). Microtiter plates were incubated at 35°C for 10 h in a Versa_{max} microplate reader (Molecular Devices, Sunnyvale, CA) set to read the absorbance at 600 nm every 10 min. Effects of EDTA concentration and metal supplementation on strains were assessed by relative growth yields and generation times (Prism 5.03; GraphPad Software, La Jolla, CA).

Purification of ZevA-His. To purify the ZevA-His fusion protein, 1-liter cultures of strain ECZevAHIS were inoculated from 10-ml overnight cultures and grown in Luria-Bertani broth containing 100 μ g/ml ampicillin with shaking at 200 rpm and 37°C. When cultures achieved an OD_{600} between 0.6 and 0.8, L-arabinose was added to a final concentration of 0.02%, and cultures were incubated for an additional 3 h. After incubation, cells were pelleted by centrifugation at $5,000 \times g$ for 10 min, resuspended in 25 mM Tris-HCl (pH 8.0) and 500 mM NaCl, and lysed using a French pressure cell. Lysates were cleared by ultracentrifugation at $30,000 \times g$, and protein was purified by affinity chromatography using a Ni^{2+} -nitrilotriacetic acid (Ni-NTA) column

(Qiagen, Valencia, CA). Protein was eluted using buffer containing 150 mM imidazole and concentrated by centrifugation in an Amicon Ultra 10-kDa cutoff filter (Millipore, Billerica, MA). To remove the His tag, ZevA-His fusion protein was incubated with purified 6×His-tagged TEV protease (1:1 molar ratio) for 1 h at 22°C in buffer containing 50 mM HEPES-NaOH (pH 7.5), 200 mM NaCl, 3 mM reduced glutathione, and 0.3 mM oxidized glutathione. After incubation, TEV-His was removed by affinity purification with Ni-NTA resin (see Fig. S1 in the supplemental material). Protein concentration was determined using the Bradford reagent (Sigma-Aldrich, St. Louis, MO). Purity was assessed by Coomassie brilliant blue staining of overloaded SDS-PAGE gels and by immunostaining Western blots with rabbit anti-His polyclonal primary antibody (GenScript, Piscataway, NJ) and goat anti-rabbit IgG secondary antibody (horseradish peroxidase conjugate; GenScript, Piscataway, NJ). Purified untagged ZevA was determined by densitometry to be at least 99% pure of ZevA-His and 98% pure of TEV-His (see Fig. S1). For Zn^{2+} binding assays, reaction buffer was exchanged with 50 mM HEPES-NaOH (pH 7.5), 200 mM NaCl, and 10% glycerol by centrifugation in an Amicon Ultra 10-kDa cutoff filter (Millipore, Billerica, MA).

Zn^{2+} binding stoichiometry determination. Stoichiometry assays were performed as described previously (18). ZevA protein (0.8 μ M) was incubated for 1 min at room temperature in the presence or absence of 50 μ M $ZnSO_4$. Buffer (50 mM HEPES-NaOH, pH 7.5, 200 mM NaCl, and 10% glycerol) containing 50 μ M $ZnSO_4$ was incubated in parallel as a control. After incubation, excess Zn^{2+} was removed by size exclusion with Sephadex G-25 columns. Eluted protein was acid digested with concentrated nitric acid overnight at room temperature. Following digestion, samples were treated with H_2O_2 to a final concentration of 1.5%. The concentration of Zn^{2+} in each sample was measured using atomic absorption spectroscopy (AAS) (AAAnalyst 300; PerkinElmer, Waltham, MA). Average background Zn^{2+} levels detected for control samples were <2% of levels determined for ZevA- Zn^{2+} samples.

Determination of ZevA affinity for Zn^{2+} . The binding affinity of ZevA for Zn^{2+} was determined using the Zn binding chromophore mag-fura-2 (Invitrogen, Carlsbad, CA) as previously described (18, 37, 67). Briefly, 10 μ M ZevA protein and 20 μ M mag-fura-2 were mixed and titrated with 1 mM Zn^{2+} . Free mag-fura-2 was determined by monitoring OD_{366} , using an ϵ_{366} of $29,900 M^{-1} cm^{-1}$ (68). Free Zn^{2+} concentrations were calculated using the equation $K_f = [Zn^{2+}]/[I_{free}][Zn^{2+}]$, where I is the concentration of mag-fura-2, I_{free} is free mag-fura-2, and K_f is the association constant of mag-fura-2 for Zn^{2+} ($K_f = 5 \times 10^7 M^{-1}$) (37, 68). The Zn^{2+} -protein association constant (K_a) and the apparent stoichiometry (n) of ZevA were calculated by fitting the data to the equation $v = nK_a[Metal]/(1 + K_a[Metal])$, where v is the ratio of moles of metal bound to total protein, n is the number of binding sites, and $[Metal]$ is the free metal concentration (25).

qRT-PCR. RNA was prepared from liquid cultures of Rd using an RNeasy minikit and an on-column DNase I kit (Qiagen, Valencia, CA). The RNA samples (5 μ g) were used as templates for cDNA synthesis with Random Primer 9 (New England BioLabs, Beverly, MA) and SuperScript II reverse transcriptase (Invitrogen, Carlsbad, CA). Quantitative reverse transcription-PCR (qRT-PCR) was performed with iQ SYBR green supermix (Bio-Rad Laboratories, Hercules, CA), and fluorescence was measured over time using the DNA Engine Opticon II system (MJ Research, Waltham, MA). For transcript analysis of *zevA* and *zevB*, qRT-PCR was performed with primers 51249RT and 31249RT and primers 51248RT and 31248RT, respectively. Primers RpoA5' and RpoA3' were used to amplify the RNA polymerase alpha subunit gene, *rpoA*, as an internal reference. The real-time cyclers conditions used have been described previously (71). The mock reverse transcription reactions, containing RNA and all reagents except reverse transcriptase, confirmed that the results obtained were not due to contaminating genomic DNAs (data not shown).

Reporter expression analysis. Strains were plated at a density of 2×10^5 CFU per plate on sBHI agar with or without 100 mM $ZnSO_4$ addition and incubated at 35°C overnight in either an open air incubator or an anaerobic chamber. Cells were swabbed from plates and diluted into Z buffer (42) to a concentration of 1×10^9 bacteria per ml (OD_{600} of 0.333). Alternatively, cells were cultured in sBHI broth containing 0.5 mM EDTA with shaking at 250 rpm and 35°C until mid-log phase before being diluted into Z buffer. The β -galactosidase (β -Gal) assay was then performed as described previously (42). The optical density at 420 nm (OD_{420}) was recorded using a Versa_{max} microplate reader (Molecular Devices, Sunnyvale, CA) and converted to Miller units with the equation Miller Units = $(1,000 \times OD_{420})/(T \times V \times OD_{600})$, where T is the time in minutes and V is the volume of the reaction mixture.

RESULTS

Identification of secreted factors involved in *H. influenzae* pathogenesis. An informatics-based approach was utilized to compile a database of the exported proteins in *H. influenzae* that are likely to require DsbA for oxidative folding. First, web-based prediction servers SignalP (7) and LipoP (32) were used to identify polypeptides with predicted cleavage sites for signal peptidase I (soluble exported proteins) and signal peptidase II (lipoproteins), respectively. Next, the list was refined to include only mature proteins (excluding leader peptides) with two or more cysteine residues, as these are expected to be DsbA substrates (50). The β -barrel outer membrane protein predictor (BOMP) (9) and membrane topology prediction servers TMHMM (63) and Phobius (33) were used to predict the locations of cysteines in the loops of membrane proteins, thereby excluding proteins with cysteines that are predicted to be cytoplasmic and inaccessible to DsbA. The final database includes secreted proteins involved in a variety of functional processes, which are cataloged based on Clusters of Orthologous Groups (COG) in Table S2 in the supplemental material.

Next, to identify the putative substrates of DsbA that are required for pathogenesis of *H. influenzae*, we cross-referenced the list of genes in Table S2 in the supplemental material with the set of genes previously implicated in survival of *H. influenzae* Rd in the lung, as identified by the HITS technique (22). In that study, transposon mutant libraries were acquired before and after selection for survival in the mouse lung model, and transposon/chromosomal junctions were amplified from genomic DNA, captured, sequenced, and aligned with the *H. influenzae* genome sequence. The results of the analysis were reported as a survival index (s.i.), which denotes the number of mutations detected in a given gene in the lung-selected output library divided by mutations detected in the *in vitro*-grown input library. Genes required during lung infection were identified on the basis of two parameters: having an s.i. of 0.3 or lower and sustaining insertions in >40% of the potential TA dinucleotide insertion sites, specific to the *himar1*-derived transposon used in the study (22). Comparison of our list of potential DsbA substrates to the results of HITS revealed three genes that fit these criteria: *znuA* (s.i., 0.101), encoding the periplasmic component of a high-affinity zinc uptake transporter (39, 53), *nlpD* (s.i., 0.000), encoding a lipoprotein suggested to be involved in daughter cell separation (64, 65), and HI1249 (s.i., 0.106), encoding a putative protein herein referred to as ZevA. The role of *znuA* in virulence has been studied by several groups (3, 11, 14, 21, 36, 57, 75), and *nlpD* has been implicated in the virulence of *Yersinia pestis* and *Yersinia enterocolitica* (12, 64). However, *znuA* has not been previously investigated and its role in virulence is unknown. Additionally, the putative gene 2 bp downstream of the 3' end of the *znuA* coding sequence, HI1248, herein referred to as *znuB*, was also found to be required for lung survival (s.i., 0.103).

The results of HITS were verified using genetic footprinting on our mutant libraries. In this technique, transposon insertions in a given region are physically mapped using PCR with a chromosome-specific primer paired with a transposon-specific primer (1, 61). The size of the amplified product corresponds to the distance between the chromosome-specific

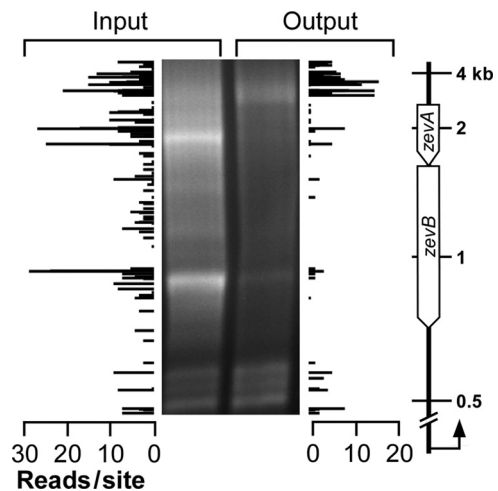


FIG. 1. Analysis of transposon insertions within the *zevAB* locus. *In vitro*-selected (Input) and *in vivo*-selected (Output) libraries were compared using HITS and genetic footprinting data. Bars represent the number of sequencing reads at each individual insertion site within the *zevAB* region. The positions of molecular weight standards are displayed to the right and apply to both HITS plots and footprints. The positions of the *zevA* and *zevB* genes are indicated. Genetic footprinting was performed by PCR with transposon-specific primer marout and chromosome-specific primer 31248rev (represented by the arrow), which binds 661 bp downstream of *zevB*.

primer and the transposon insertion within that gene. In agreement with HITS, footprints of the library recovered from lung infection reveal a reduction in transposon insertions within the *zevAB* locus compared with footprints of the input library (Fig. 1). These data indicate that *zevA* and *zevB* are essential for lung colonization by *H. influenzae* Rd.

***zevAB* is required for efficient NTHI infection of the mouse lung.** Mutants of *zevA* and *zevB* were generated in an NTHI clinical isolate, NT127 (28), to evaluate the roles of these genes during *in vitro* growth and lung infection. Mutants were constructed by replacement of coding regions with a drug resistance marker to generate nonpolar deletions, and complementation was conducted using an exchange vector for delivery and expression at the xylose locus (70). The complete strain set consisted of the parent strain carrying the empty vector (NTV), the *zevA* mutant carrying the empty vector (NTzevAV), the *zevB* mutant carrying the empty vector (NTzevBV), and complemented *zevA* and *zevB* mutants (NTzevAX and NTzevBX, respectively) (Table 1). When grown aerobically in sBHI medium, all strains had equivalent growth yields and generation times (NTV, 45.4 ± 1.7 min; NTzevAV, 44.1 ± 1.3 min; NTzevBV, 41.6 ± 0.6 min; NTzevAC, 43.0 ± 0.5 min; and NTzevBC, 44.2 ± 1.9 min). Ratios of CFU to optical densities at 600 nm were indistinguishable between these strains.

Next, these strains were evaluated for their ability to infect the lungs of C57BL/6 mice. This experiment was performed using mixed infections in which a competition was performed between each strain and strain NTlacZ, which expresses *E. coli lacZ* at the *xyl* locus. At 40 h after inoculation, average competitive indices (c.i.) were ~ 3 -fold lower for the *zevA* mutant (NTzevAV; c.i., 0.364) and ~ 22 -fold lower for the *zevB* mutant (NTzevBV; c.i., 0.064) compared to that for the parent strain (NTV; c.i., 1.22) (Fig. 2). Complementation restored the ability

TABLE 1. Strains and plasmids used in this study

Strain or plasmid	Genotype, description, and/or relevant features	Reference or source
Strains		
NT127	Nontypeable <i>H. influenzae</i> clinical isolate	28
NTV	NT127 <i>xylA</i> Δ_{4-804} :: <i>tetAR</i> ; <i>tetAR</i> sequence from pXT10 replaces <i>xylA</i>	28
NTzevAV	NT127 Δ <i>zevA</i> :: <i>aacCI</i> , <i>xylA</i> Δ_{4-804} :: <i>tetAR</i> ; <i>zevA</i> deletion mutant with <i>tetAR</i> Tc ^r cassette replacing <i>xylA</i>	This study
NTzevAX	NT127 Δ <i>zevA</i> :: <i>aacCI</i> ; <i>xylA</i> Δ_{4-804} :: <i>zevA</i> ; <i>zevA</i> deletion mutant complemented with <i>zevA</i> expressed via the <i>zevA</i> promoter in place of <i>xylA</i>	This study
NTzevBV	NT127 Δ <i>zevB</i> :: <i>aacCI</i> ; <i>xylA</i> Δ_{4-804} :: <i>tetAR</i> ; <i>zevA</i> mutant replacing <i>xylA</i>	This study
NTzevBX	NT127 Δ <i>zevB</i> :: <i>aacCI</i> ; <i>xylA</i> Δ_{4-804} :: <i>zevAB</i> ; <i>zevB</i> deletion mutant complemented with <i>zevAB</i> expressed via the <i>zevA</i> promoter in place of <i>xylA</i>	This study
NTlacZ	NT127 <i>xylA</i> Δ_{4-804} :: <i>lacZ</i> ; <i>lacZ</i> coding sequence expressed via the <i>xylA</i> promoter replacing <i>xylA</i>	This study
NTznuA	NT127 Δ <i>znuA</i> :: <i>aphI</i> , <i>xylA</i> Δ_{4-804} :: <i>tetAR</i> ; <i>znuA</i> deletion mutant with <i>tetAR</i> Tc ^r cassette replacing <i>xylA</i>	This study
NTzevAznuA	NTzevAV Δ <i>znuA</i> :: <i>aphI</i> ; <i>zevA</i> and <i>znuA</i> double mutants	This study
NTzevBznuA	NTzevBV Δ <i>znuA</i> :: <i>aphI</i> ; <i>zevB</i> and <i>znuA</i> double mutants	This study
NTznuB	NT127 Δ <i>znuBC</i> :: <i>aphI</i> , <i>xylA</i> Δ_{4-804} :: <i>tetAR</i> ; <i>znuBC</i> deletion mutant with <i>tetAR</i> Tc ^r cassette replacing <i>xylA</i>	This study
NTzevAznuBC	NTzevAV Δ <i>znuBC</i> :: <i>aphI</i> ; <i>zevA</i> and <i>znuBC</i> double mutants	This study
NTzevBznuBC	NTzevBV Δ <i>znuBC</i> :: <i>aphI</i> ; <i>zevB</i> and <i>znuBC</i> double mutants	This study
Rd AW	Wild type; <i>H. influenzae</i> capsule-deficient type d	70
R5	Rd Δ <i>zevAB</i> :: <i>lacZ</i> ; <i>zevAB</i> deletion mutant with <i>lacZ</i> expressed via the <i>zevA</i> promoter (<i>zevA</i> reporter strain)	This study
R5X	R5 <i>xylA</i> Δ_{4-804} :: <i>zevAB</i> ; strain R5 complemented with <i>zevAB</i> expressed via the <i>zevA</i> promoter replacing <i>xylA</i>	This study
R5fnr	R5 <i>fnr</i> :: <i>nptIII</i> ; <i>fnr</i> mutant of strain R5 with Km ^r transposon insertion in <i>fnr</i>	This study
R5fnrX	R5 <i>fnr</i> <i>xylA</i> Δ_{4-804} :: <i>fnr</i> ; <i>fnr</i> mutant of strain R5 complemented with <i>fnr</i> expressed via the <i>fnr</i> promoter in place of <i>xylA</i>	This study
RdlacZ	Rd <i>xylA</i> Δ_{4-804} :: <i>lacZ</i> ; <i>lacZ</i> coding sequence expressed via the <i>trc</i> promoter replacing <i>xylA</i>	71
Plasmids		
pXT10	Delivery vector for chromosomal expression at the xylose locus of <i>H. influenzae</i> containing <i>xylF</i> , <i>xylB</i> , <i>xylA</i> Δ_{4-804} , and the <i>tetAR</i> tetracycline resistance cassette	70
P1249J	pXT10 carrying <i>zevA</i> from NT127 expressed from the <i>zevA</i> promoter	This study
p1248J1	pXT10 carrying <i>zevAB</i> from NT127 expressed from the <i>zevA</i> promoter	This study
pX1248R	pXT10 carrying <i>zevAB</i> from Rd expressed from the <i>zevA</i> promoter	This study
pXELacZ2	pXT10 carrying <i>lacZ</i> expressed from the <i>xylA</i> promoter	This study

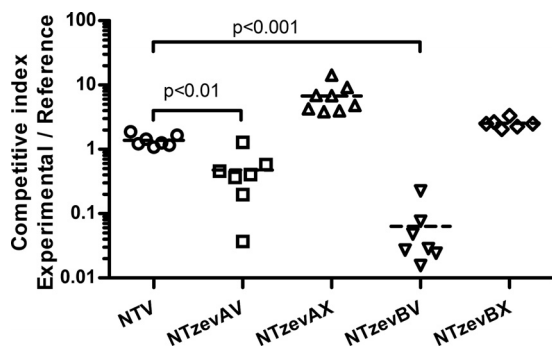


FIG. 2. Effect of *zevA* and *zevB* mutations on survival of NTHI in the mouse lung infection model. Mice were coinoculated with reference strain NTlacZ and the parent strain carrying the empty vector (NTV), the *zevA* mutant (NTzevAV), the complemented *zevA* mutant (NTzevAX), the *zevB* mutant (NTzevBV), or the complemented *zevB* mutant (NTzevBX). Bacteria were recovered from lung homogenates after 40 h. Competitive indices (c.i.) are calculated as the ratio of recovered CFU of the LacZ⁻ experimental strain to recovered CFU of the LacZ⁺ reference strain. The symbols indicate data for individual animals, and the dashed lines indicate averages. The lower limit of detection was a c.i. of 0.001. Relevant statistical comparisons are indicated by brackets, and *P* values were determined using ANOVA with Tukey's multiple-comparison test. NTV, *n* = 8; NTzevAV, *n* = 7; NTzevAX, *n* = 8; NTzevBV, *n* = 7; NTzevBX, *n* = 6.

of the mutants to survive in the lung, verifying that defects are specific to mutation of *zevA* and *zevB*. The complemented strains, NTzevAX and NTzevBX, exhibited competitive indices that were slightly higher than that of the parent strain, likely due to increased expression of the complementing genes due to the presence of both the *zevA* and *xylA* promoters in the constructs. To examine the possibility that mixed infection influences relative survival of the mutants, the *zevA* mutant was evaluated in the lung model in single-strain infections. Consistent with results obtained with mixed infections, average CFU recovery at 40 h postinfection was significantly reduced (*P* = 0.027) 3.5-fold for the *zevA* mutant compared to that for the parent strain (data not shown). In agreement with HITS analysis of Rd, these data indicate that the *zevAB* genes are required for colonization and survival of pathogenic NTHI in the mouse lung but are not required for normal growth in rich medium.

Bioinformatic analysis of *zevA* and *zevB*. BLAST (2) reveals that *zevA* and *zevB* of *H. influenzae* are conserved in other bacterial species within the *Pasteurellaceae* and *Enterobacteriaceae*, including several human pathogens such as *Klebsiella pneumoniae*, *Yersinia pestis*, *Proteus mirabilis*, and *Salmonella enterica* serovar Typhimurium (Table 2). In the Conserved Domains Database (CDD) (40), ZevA and ZevB are annotated by structural domain classification as the periplasmic substrate-binding protein (PBP) and the permease subunit of

TABLE 2. BLAST results of *H. influenzae* Rd ZevA and ZevB homologs in other pathogens^a

Organism	ZevA (HI1249)				ZevB (HI1248)			
	Locus ID	Identity (%)	Length (aa)	Expect value	Locus ID	Identity (%)	Length (aa)	Expect value
<i>H. influenzae</i> NT127	HIAG_01363	97	206	2e-117	HIAG_01364	96	322	5e-165
<i>Klebsiella pneumoniae</i> 342	Kpk_1251	42	199	7e-42	Kpk_1252	36	326	2e-40
<i>Yersinia pestis</i> KIM 10	y1329	43	224	3e-41	y1330	38	340	7e-52
<i>Proteus mirabilis</i> HI4320	PMI1519	37	221	2e-32	PMI1518	38	333	8e-47
<i>Salmonella enterica</i> serovar Typhimurium LT2	STM2552	37	212	1e-33	STM2551	38	328	1e-50

^a ID, identification. HI1249, 206 amino acids (aa); HI1248, 322 (aa).

an ATP-binding cassette (ABC) transporter, respectively. ZevB is also annotated as a member of the NiCoT superfamily of potential nickel/cobalt importers and exporters (2). This superfamily is comprised of a diverse group of eight transmembrane segmented secondary transporters with a characteristic HX₄DH sequence in their second transmembrane span (17). ZevB does not show these characteristics. Moreover, modeling of ZevB using the consensus prediction of membrane protein topology server (TOPCONS) (8) indicates that it contains only the typical six transmembrane spans present in each of the two transmembrane subunits observed in ABC ATPases (13). This evidence suggests that ZevA and ZevB are partnering components of an ABC ATPase transport system probably involved in substrate influx.

ZevA and ZevB are important for growth of *H. influenzae* during zinc limitation. Metal-restricted growth conditions can be generated by titration of the medium with increasing concentrations of EDTA (3, 11, 54). To determine whether *zevAB* is involved in metal acquisition in *H. influenzae*, strains were grown in medium containing 0.25, 0.5, or 0.75 mM EDTA. Mutants of *zevA* and *zevB* were able to acquire essential nutrients for optimal growth in rich medium, as evidenced by the lack of apparent growth defects *in vitro* (Fig. 3A). However, medium containing 0.5 mM EDTA inhibited growth of the *zevA* and *zevB* mutants, in which growth yields at 10 h were reduced by 81% and 87%, respectively, compared to that of the parent or complemented strains, which grew normally (Fig. 3B). Supplementation with 0.25 mM EDTA had no effect on the growth of any strains, whereas 0.75 mM EDTA significantly reduced growth of the parent and complemented strains in addition to that of the mutants (data not shown).

In preliminary studies, specific metals were added to medium chelated with EDTA in an attempt to promote growth of the mutants. The addition of MgCl₂, CaCl₂, MnCl₂, FeCl₃, CoCl₂, NiCl₂, CuSO₄, or Na₂MoO₄ at a concentration of either 30 or 60 μM had no significant effect on the growth of the *zevB* mutant in the presence of 0.5 mM EDTA (data not shown). In contrast, addition of 30 μM ZnSO₄ partially restored the growth of the *zevB* mutant and addition of 60 μM ZnSO₄ completely restored growth to the level of the parent strain. Figure 3C shows that in the presence of 0.5 mM EDTA, addition of 60 μM zinc restores both the *zevA* and *zevB* mutants to levels of the parent and complemented strains. These data suggest that *zevAB* is important for the growth of *H. influenzae* under conditions where free zinc is limiting.

ZevA protein binds zinc with high affinity. Metal binding assays were performed to determine whether ZevA binds Zn²⁺

and therefore can participate in metal uptake. Recombinant ZevA was cloned, expressed in *Escherichia coli*, and affinity purified, and the metal binding tag was removed. After incubation in the presence of Zn²⁺, the amount of metal bound to ZevA was determined by atomic absorption spectroscopy (AAS). The results indicate that ZevA binds 1.9 ± 0.3 Zn²⁺ ions per mol of ZevA. The affinity of ZevA for Zn²⁺ was determined in metal competition assays including ZevA and mag-fura-2. The fluorescent metal chelator mag-fura-2 binds

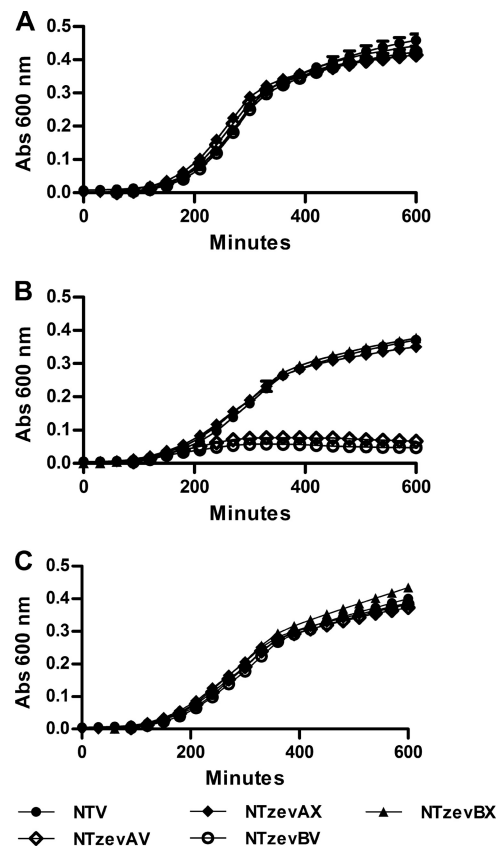


FIG. 3. Growth phenotypes of *zevA* and *zevB* mutants in liquid medium. The parent strain (NTV), *zevA* mutant (NTzevAV), complemented *zevA* mutant (NTzevAX), *zevB* mutant (NTzevBV), and complemented *zevB* mutant (NTzevBX) were grown in sBHI (A), sBHI containing 0.5 mM EDTA (B), or sBHI containing 0.5 mM EDTA supplemented with 60 μM ZnSO₄ (C). Symbols represent average absorbance (Abs) readings for three cultures. Error bars indicate standard deviations (SD).

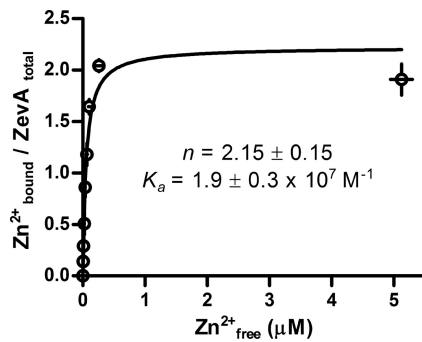


FIG. 4. Zn^{2+} binding to purified recombinant ZevA. The association constant (K_a) and the number of metal binding sites (n) of ZevA were calculated by fitting the data to the equation $v = nK_a[Metal]/(1 + K_a[Metal])$, where v is the ratio of moles of metal bound to total protein and n is the number of binding sites. Symbols represent the averages of three independent measurements, and error bars indicate standard errors.

Zn^{2+} with a K_a of $5 \times 10^7 M^{-1}$, and this is associated with a shift from 366 nm to 325 nm in the chelator's spectrum maximum. Thus, the decrease in OD_{366} was used to calculate the concentrations of the various species in the assay. Figure 4 shows the results of these assays. Cooperativity in binding to the two Zn^{2+} binding sites was not observed. Fitting the data to a Langmuir equation yielded an association constant of ZevA for Zn^{2+} of $1.9 \times 10^7 \pm 0.3 \times 10^7 M^{-1}$. This affinity is similar to those observed for other known Zn^{2+} binding proteins (15, 24, 37).

Relative contributions of *zevAB* and *znuABC* in zinc utilization. Aside from the ZevAB system presented here, only one other system has been implicated in zinc utilization of *H. influenzae*, the high-affinity zinc transporter ZnuABC. An *H. influenzae znuA* (originally called *pzp1*) mutant was shown to exhibit growth defects in normal medium that could be rescued by addition of zinc, and recombinant ZnuA bound up to 5 molecules of zinc per protein (39). The *znuBC* genes have also been demonstrated to participate in zinc utilization in other organisms (11, 53), including *Pasteurella multocida* (21), a close relative of *H. influenzae*, and are thought to encode the ATPase (*znuC*) and membrane permease (*znuB*) components of the transporter (52, 53). To evaluate the conditions under which ZevAB and ZnuABC are needed, their relative contributions to the growth of *H. influenzae* were examined through single and double mutant analyses. First, a *znuA* mutant was generated by replacement of its coding region with an antibiotic resistance marker, and its growth was compared to that of the *zevA* and *zevB* mutants. The *znuA* mutant (NTznuA) exhibited an ~16% increase in generation time in sBHI broth relative to the parent strain (NTV), *zevA* mutant (NTzevAV), and *zevB* mutant (NTzevBV) (Fig. 5A). Addition of 60 μM zinc restored growth of the *znuA* mutant in rich medium to wild-type levels (data not shown), similar to results previously reported for *znuA* mutants of other *H. influenzae* strains (39). When grown in 0.1 mM EDTA, the *znuA* mutant exhibited both a 21-fold reduction in growth yield at 10 h and a 2.3-fold increase in generation time compared with growth of this strain in sBHI medium, whereas the parent strain, *zevA* mutant, and *zevB* mutant grew normally under this condition (Fig.

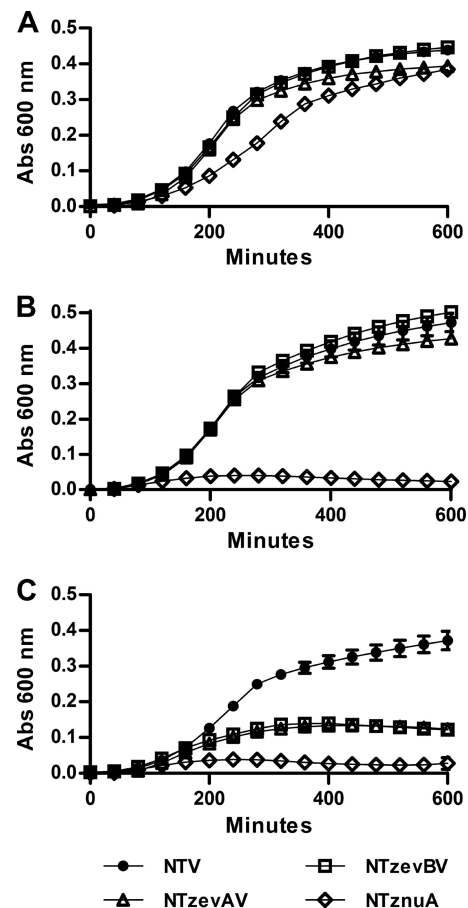


FIG. 5. Growth phenotypes of *zevA*, *zevB*, and *znuA* mutants in liquid medium. The parent strain (NTV), *zevA* mutant (NTzevAV), *zevB* mutant (NTzevBV), and *znuA* mutant (NTznuA) were grown in sBHI (A), sBHI containing 0.1 mM EDTA (B), or sBHI containing 0.5 mM EDTA (C). Symbols represent average absorbance (Abs) readings for three cultures. Error bars indicate SD.

5B). In the presence of 0.5 mM EDTA, the growth yield of the *znuA* mutant was also reduced 21-fold compared to that of the parent strain (Fig. 5C). Additionally, growth yields of the *zevA* and *zevB* mutants were reduced by 67% compared with that of the parent strain, similar to data reported for these strains in Fig. 3B. A *znuBC* deletion, which was also constructed by gene replacement, exhibited defects similar to those of the *znuA* mutant during growth in rich medium or medium containing 0.5 mM EDTA (data not shown), providing evidence that ZnuBC functions together with ZnuA in NTHI as components of the zinc transport system described previously for other organisms (11, 21, 53).

Next, to examine the role of *zevAB* in zinc uptake in the absence of the *znuABC* pathway, double mutants were generated by deletion of *znuA* or *znuBC* in either the *zevA* or *zevB* mutant background. The growth phenotypes of the double mutants were equal in severity to that of the *znuA* or *znuBC* mutant in sBHI medium, sBHI with various concentrations of EDTA (0.0025 mM, 0.005 mM, or 0.01 mM), or sBHI supplemented with various concentrations of zinc (0.001 mM, 0.003 mM, or 0.05 mM). The lack of an additive effect of *zevA* or

zevB mutation in combination with *znuA* or *znuBC* mutation indicates that ZevAB does not substitute for ZnuABC for zinc uptake at these zinc concentrations. Taken together, these data suggest that ZevAB functions in a specialized pathway needed only when the concentration of free zinc is low in contrast to that of ZnuABC, which is essential for growth over a wide range of free zinc concentrations.

FNR participates in regulation of the ZevAB operon. In many species that have been examined, transcriptional regulation of bacterial genes involved in zinc uptake is mediated by the zinc-responsive metalloregulatory protein Zur (27). When zinc is abundant in the cell, dimerized Zur binds to a specific palindromic sequence in promoters to repress transcription of zinc uptake genes, such as *znuABC* of *E. coli* (53) and *zinT* of *S. Typhimurium* (54). However, previous studies, as well as our own BLAST searches, indicate that the *Pasteurellaceae* do not contain a *zur* homolog (21). In these organisms, zinc uptake is likely regulated by other mechanisms. For example, in *Pasteurella multocida*, *znuABC* is regulated by the iron response regulator Fur (21).

To investigate the potential regulation of *zevAB*, the 330-bp region directly upstream of the *zevA* translational start site from the start codon of HI1250 (negative strand relative to the *zevA* coding sequence) to the start codon of *zevA* (positive strand) was analyzed for potential transcriptional regulator binding sites. A palindromic sequence between 235 and 248 bp upstream of the HI1250 start codon that was conserved in both Rd and NT127 strains was identified (Fig. 6A). This sequence matches the known consensus binding site for the oxygen-responsive transcriptional regulator FNR (16, 41). FNR directly senses a range of low-oxygen conditions and binds to DNA to either repress genes required for aerobic growth or activate those needed for growth under low-oxygen conditions (28, 35).

To determine the expression profiles of *zevA* and *zevB*, we first examined the transcription of these genes in the Rd strain. Cultures were grown in liquid medium, and transcript levels were determined by quantitative PCR, revealing that *zevA* and *zevB* are expressed similarly to the reference gene *rpoA*, which encodes RNA polymerase. Together with their genomic organization, these data suggest that *zevA* and *zevB* may be expressed via the same promoter.

Next, to determine whether the *zevAB* genes are regulated in response to oxygen, reporter strain R5 was constructed as a *zevA* promoter-*lacZ* fusion with deletion of *zevAB* in the Rd background (Fig. 6A). A complemented reporter strain, R5X, was also generated in which the *zevAB* genes were expressed via their native promoter at the *xyl* locus in *trans* to the *zevA* promoter-*lacZ* fusion. When grown aerobically (sBHI agar plate), β -Gal activities were similar between the reporter strain, R5, and the complemented reporter strain, R5X (Fig. 6B). When bacteria were grown anaerobically, β -Gal activities were reduced for both strains by $\sim 50\%$ compared with aerobic levels. A strain carrying an *fnr* disruption mutation in the R5 background, R5fnr, exhibited $\sim 80\%$ greater β -Gal activity than the parent reporter strain or complemented reporter strain under anaerobic conditions, effectively restoring activity to levels observed for the parent strain under aerobic conditions. The *fnr* mutant also exhibited an $\sim 25\%$ increase in β -Gal activity compared with the parent strain under aerobic

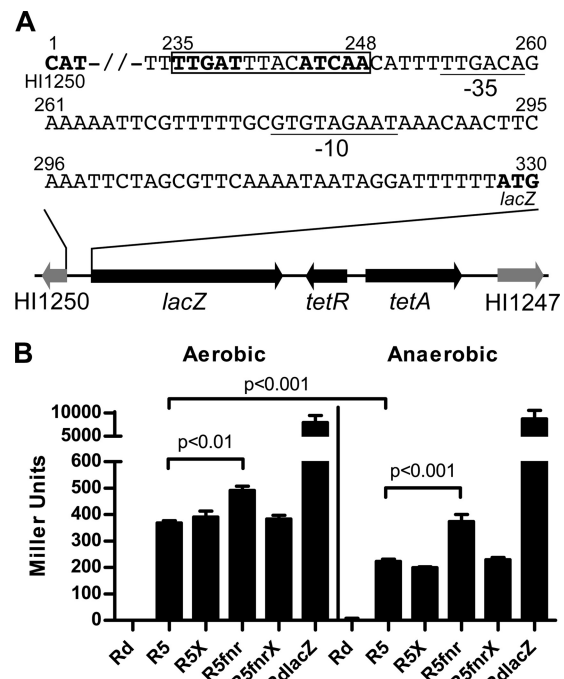


FIG. 6. FNR-mediated regulation of the *zevA* promoter. (A) Schematic of *zevA* promoter-*lacZ* fusion construct inserted into the Rd genome at the *zevAB* locus. The 330-bp intergenic region from the start codon of HI1250 to the start codon of *lacZ* is displayed above. A potential FNR binding site is indicated by a box, and bold letters indicate the palindromic sequence. The predicted -10 and -35 promoter elements are underlined. (B) β -Galactosidase activity. The parent strain (Rd), reporter strain (R5), complemented reporter strain (R5X), reporter strain carrying an *fnr* mutation (R5fnr), complemented *fnr* mutant (R5fnrX), and positive-control strain (RdlacZ) were plated at a density of 5×10^8 CFU, grown in aerobic and anaerobic environments, and assayed for the production of β -galactosidase. Values are displayed in Miller units. Relevant statistical comparisons are indicated by brackets, and *P* values were determined using ANOVA with Tukey's multiple-comparison test. Bars represent average measurements for three technical replicates. Error bars indicate SD.

conditions, likely due to oxygen availability decreasing as culture density increases on the plate. Complementation restored levels of fusion expression in the *fnr* mutant to those of the wild type. Additionally, RdlacZ, a strain expressing *lacZ* via a constitutive promoter, produced equivalent β -Gal levels in both the aerobic and anaerobic environments, suggesting that β -Gal activity itself is not affected by the growth condition (Fig. 6B).

To examine whether free zinc concentrations affect *zevA* reporter expression, the complemented reporter strain, R5X, was grown in liquid medium in the presence or absence of 0.5 mM EDTA under aerobic conditions. In this assay, β -Gal levels of R5X were indistinguishable between the two conditions (data not shown). When R5X was grown under either aerobic or anaerobic conditions in medium supplemented with 100 mM zinc (a concentration nontoxic to *H. influenzae*), β -Gal levels were similar to those observed for this strain in normal sBHI medium (data not shown). Taken together, these data indicate that expression from the *zevA* promoter is unaffected by the presence or absence of *zevAB* or changes in free zinc concentrations and is repressed by FNR under oxygen-limiting

conditions. Furthermore, a higher level of *zevA* promoter activity in the aerobic environment is consistent with the requirement of *zevAB* for lung infection, in which *H. influenzae* is likely to encounter high oxygen concentrations.

DISCUSSION

Secreted bacterial proteins mediate critical aspects of pathogenesis and often require disulfide bond formation in the periplasm to stabilize their mature structures. Due to their extracytoplasmic location and accessibility, identification of these factors may aid in the design of novel therapeutics or vaccines for combating NTHI infections. Here, we generated a list of potential substrates of the periplasmic disulfide oxidoreductase protein DsbA (see Table S2 in the supplemental material) and integrated our findings with the results of a previous study in which HITS technology was used to identify genes required for lung infection (22). Using this strategy, we identified three genes that were potentially important for lung infection, including two, *znuA* and *nlpD*, that had previously been implicated in the virulence of several organisms (3, 11, 12, 14, 21, 36, 57, 64, 75), and a third gene, *zevA*, whose function had not been determined. Therefore, *zevA* and its neighboring gene, *zevB*, were investigated for their roles in the pathogenesis of a clinical NTHI isolate. NTHI mutants of *zevA* and *zevB* were not defective for growth *in vitro* on rich medium compared with the parent or complemented strain but exhibited significant survival defects in a mouse lung infection model (Fig. 2). These data confirmed that *zevA* and *zevB* are indispensable for the virulence of *H. influenzae* strains in the murine lung. Interestingly, several potential DsbA-dependent proteins that were not required in the lung model as determined by HITS are important for *H. influenzae* pathogenesis in other sites of infection. For example, the hemopexin utilization protein HxuA has been shown to be required for wild-type bacteremic levels in an infant rat model of *H. influenzae* type B infection (45), and the outer membrane protein P5 (OmpA) is required for virulence of NTHI in a chinchilla model of otitis media (62). This suggests that examination of the requirement for DsbA substrates in other *H. influenzae* infection models is likely to reveal additional mechanisms involved in pathogenesis.

Informatics-based analysis of ZevAB suggested potential roles in metal transport, and this possibility was explored. Mutants of *zevA* and *zevB* were highly defective for growth in the presence of 0.5 mM EDTA (Fig. 3B), suggesting that these genes are important during metal-restricted growth. Supplementation with 60 μ M zinc, but not other metals, was able to rescue the growth of the *zevA* and *zevB* mutants in the presence of 0.5 mM EDTA to levels of the parent and complemented strains (Fig. 3C). The concentration of zinc in sBHI medium was determined to be 40 μ M using AAS. Therefore, upon chelation with EDTA, addition of 60 μ M likely restores free zinc concentrations to the normal range found in sBHI media. Together, these data indicate that *zevAB* is a novel zinc utilization pathway important for growth of *H. influenzae* when free zinc concentrations are limiting. Consistent with this observation, we also demonstrated that ZevA protein binds to two zinc ions with high affinity (Fig. 4), similar to periplasmic binding proteins of other high-affinity zinc transporters (15, 24).

H. influenzae encodes at least two zinc utilization systems, the ZnuABC system and the ZevAB system described here. Mutants of individual genes in both pathways were compared for growth levels in rich or metal-restricted medium, and growth defects of the *znuA* mutant were consistently more severe than defects exhibited by the parent strain or *zevA* or *zevB* mutant in rich medium or medium containing EDTA (Fig. 5A, B, and C). These data are consistent with the role of ZnuABC as a primary zinc transport system of *H. influenzae*, required over a wide range of conditions, whereas contributions from ZevAB are important for supporting growth only when zinc concentrations are limiting. Because double mutant analysis revealed that strains lacking both Znu and Zev pathways are not completely inhibited for growth in rich medium, it is likely that an additional pathway is involved in zinc acquisition of this organism. One possibility is the PitA-dependent inorganic phosphate utilization pathway, which was proposed to be a low-affinity zinc transporter of *E. coli* (6). Whole-genome mutant fitness analysis via HITS suggested that PitA is required for optimal growth *in vitro* as well as for lung infection (22). Together, these observations suggest that *H. influenzae* contains several zinc utilization pathways whose functions are specialized to maintain zinc homeostasis in diverse environments.

Consistent with our observation that these proteins participate in zinc utilization, bioinformatic analysis of ZevA and ZevB suggested that they constitute PBP and membrane permease components of an ABC-type transporter, respectively. However, the *zevAB* locus does not encode a protein containing the Walker A and B nucleotide binding sequences known to be required by ABC transporters for activity (13). HITS analysis revealed seven genes required for lung infection that are predicted to encode ABC-type ATPases (22). Possibly, ZevAB utilizes one of these ATPases for function; however, further investigation will be needed to address this question.

In many bacterial species, genes important for zinc acquisition and homeostasis are repressed in response to elevated intracellular zinc levels by the transcriptional regulator Zur (27, 54). Because *H. influenzae* does not contain a homolog of this regulator and expression of *zevAB* was not influenced by exogenous zinc levels, we sought to determine whether another regulator was involved. Expression analysis using *zevA* promoter-*lacZ* fusion reporter strains revealed that *zevAB* is repressed under low-oxygen conditions by the oxygen-responsive transcriptional regulator FNR (Fig. 6B). Of note, FNR has been shown to positively regulate transcription of metal transporters, such as *nikABCDE* nickel transport genes and *feoABC* iron uptake genes of *E. coli* (34, 73) and *feoABC*, *sitABCD*, and *fhuA* iron uptake genes of *Shigella flexneri* (10, 74). To our knowledge, FNR-mediated regulation of genes involved in zinc acquisition or homeostasis has not previously been demonstrated.

A potential explanation for the repression of *zevAB* by FNR is that maximum expression of *zevAB* may be detrimental to the survival of *H. influenzae* in the anaerobic environment due to excessive zinc uptake or that *zevAB* may be dispensable during anaerobic growth and repressed to conserve resources. However, an *fnr* mutant and a wild-type strain were equally sensitive to a range of toxic zinc concentrations during anaerobic growth, and defects in the growth of a *zevB* mutant in

zinc-limiting medium were not significantly different under aerobic and anaerobic conditions (C. V. Rosadini, unpublished results). Ultimately, regulation of *zevAB* by FNR may serve as an important strategy for increasing this system's expression exclusively in sites of infection where the bacterium encounters zinc limitation, as is likely to occur at airway mucosal surfaces, and is consistent with other reports indicating that oxygen is an important signal for modulation of virulence factor expression in *H. influenzae* (69, 71, 72).

Bacteria are thought to contain high-affinity zinc transporters as a strategy to overcome zinc limitation during infection in which the acute phase response has been shown to result in reduced plasma zinc concentrations (20, 38) with upregulation and release of the zinc binding complex calprotectin in the blood and lungs (29, 31, 55). In accord with this hypothesis, we demonstrated here that *H. influenzae* requires a specialized high-affinity zinc utilization pathway for virulence. The finding that *zevAB* is needed exclusively during growth under low-zinc conditions and is required for lung infection suggests that bacteria growing in the lung experience zinc limitation that may represent an immune defense for controlling pulmonary infection.

ACKNOWLEDGMENTS

This work was supported by NIH grants 2R56AI049437-07 (B.J.A.) and 1R21AI082484-01 (J.M.A.).

We thank Don Pellegrino for his valuable assistance with AAS determinations.

REFERENCES

- Akerley, B. J., and D. J. Lampe. 2002. Analysis of gene function in bacterial pathogens by GAMBIT. *Methods Enzymol.* **358**:100–108.
- Altschul, S. F., W. Gish, W. Miller, E. W. Myers, and D. J. Lipman. 1990. Basic local alignment search tool. *J. Mol. Biol.* **215**:403–410.
- Ammendola, S., et al. 2007. High-affinity Zn²⁺ uptake system ZnuABC is required for bacterial zinc homeostasis in intracellular environments and contributes to the virulence of *Salmonella enterica*. *Infect. Immun.* **75**:5867–5876.
- Ausubel, F. M., et al. (ed.). 1995. *Current protocols in molecular biology*. John Wiley & Sons, Inc., New York, NY.
- Barcak, G. J., M. S. Chandler, R. J. Redfield, and J. F. Tomb. 1991. Genetic systems in *Haemophilus influenzae*. *Methods Enzymol.* **204**:321–342.
- Beard, S. J., et al. 2000. Evidence for the transport of zinc(II) ions via the Pit inorganic phosphate transport system in *Escherichia coli*. *FEMS Microbiol. Lett.* **184**:231–235.
- Bendtsen, J. D., H. Nielsen, G. von Heijne, and S. Brunak. 2004. Improved prediction of signal peptides: SignalP 3.0. *J. Mol. Biol.* **340**:783–795.
- Bernsel, A., H. Viklund, A. Hennerdal, and A. Elofsson. 2009. TOPCONS: consensus prediction of membrane protein topology. *Nucleic Acids Res.* **37**:W465–W468.
- Berven, F. S., K. Flikka, H. B. Jensen, and I. Eidhammer. 2004. BOMP: a program to predict integral beta-barrel outer membrane proteins encoded within genomes of Gram-negative bacteria. *Nucleic Acids Res.* **32**:W394–W399.
- Boulette, M. L., and S. M. Payne. 2007. Anaerobic regulation of *Shigella flexneri* virulence: ArcA regulates Fur and iron acquisition genes. *J. Bacteriol.* **189**:6957–6967.
- Campoy, S., et al. 2002. Role of the high-affinity zinc uptake *znuABC* system in *Salmonella enterica* serovar Typhimurium virulence. *Infect. Immun.* **70**:4721–4725.
- Darwin, A. J., and V. L. Miller. 1999. Identification of *Yersinia enterocolitica* genes affecting survival in an animal host using signature-tagged transposon mutagenesis. *Mol. Microbiol.* **32**:51–62.
- Davidson, A. L., E. Dassa, C. Orelle, and J. Chen. 2008. Structure, function, and evolution of bacterial ATP-binding cassette systems. *Microbiol. Mol. Biol. Rev.* **72**:317–364.
- Davis, L. M., T. Kakuda, and V. J. DiRita. 2009. A *Campylobacter jejuni* *znuA* orthologue is essential for growth in low-zinc environments and chick colonization. *J. Bacteriol.* **191**:1631–1640.
- Desrosiers, D. C., et al. 2007. The general transition metal (Tro) and Zn²⁺ (Znu) transporters in *Treponema pallidum*: analysis of metal specificities and expression profiles. *Mol. Microbiol.* **65**:137–152.
- Eiglmeier, K., N. Honore, S. Iuchi, E. C. Lin, and S. T. Cole. 1989. Molecular genetic analysis of FNR-dependent promoters. *Mol. Microbiol.* **3**:869–878.
- Eitinger, T., J. Suhr, L. Moore, and J. A. Smith. 2005. Secondary transporters for nickel and cobalt ions: theme and variations. *Biometals* **18**:399–405.
- Eren, E., D. C. Kennedy, M. J. Maroney, and J. M. Arguello. 2006. A novel regulatory metal binding domain is present in the C terminus of Arabidopsis Zn²⁺-ATPase HMA2. *J. Biol. Chem.* **281**:33881–33891.
- Frech, C., M. Wunderlich, R. Glockshuber, and F. X. Schmid. 1996. Preferential binding of an unfolded protein to DsbA. *EMBO J.* **15**:392–398.
- Gabay, C., and I. Kushner. 1999. Acute-phase proteins and other systemic responses to inflammation. *N. Engl. J. Med.* **340**:448–454.
- Garrido, M. E., et al. 2003. The high-affinity zinc-uptake system *znuACB* is under control of the iron-uptake regulator (*fur*) gene in the animal pathogen *Pasteurella multocida*. *FEMS Microbiol. Lett.* **221**:31–37.
- Gawronski, J. D., S. M. Wong, G. Giannoukos, D. V. Ward, and B. J. Akerley. 2009. Tracking insertion mutants within libraries by deep sequencing and a genome-wide screen for *Haemophilus* genes required in the lung. *Proc. Natl. Acad. Sci. U. S. A.* **106**:16422–16427.
- Gilligan, P. H. 1991. Microbiology of airway disease in patients with cystic fibrosis. *Clin. Microbiol. Rev.* **4**:35–51.
- Graham, A. L., et al. 2009. Severe zinc depletion of *Escherichia coli*: roles for high affinity zinc binding by ZinT, zinc transport and zinc-independent proteins. *J. Biol. Chem.* **284**:18377–18389.
- Guo, J., and D. P. Giedroc. 1997. Zinc site redesign in T4 gene 32 protein: structure and stability of cobalt(II) complexes formed by wild-type and metal ligand substitution mutants. *Biochemistry* **36**:730–742.
- Hanson, M. S., C. Slaughter, and E. J. Hansen. 1992. The *hbpA* gene of *Haemophilus influenzae* type b encodes a heme-binding lipoprotein conserved among heme-dependent *Haemophilus* species. *Infect. Immun.* **60**:2257–2266.
- Hantke, K. 2005. Bacterial zinc uptake and regulators. *Curr. Opin. Microbiol.* **8**:196–202.
- Harrington, J. C., et al. 2009. Resistance of *Haemophilus influenzae* to reactive nitrogen donors and gamma interferon-stimulated macrophages requires the formate-dependent nitrite reductase regulator-activated *ytfE* gene. *Infect. Immun.* **77**:1945–1958.
- Henke, M. O., et al. 2006. Up-regulation of S100A8 and S100A9 protein in bronchial epithelial cells by lipopolysaccharide. *Exp. Lung Res.* **32**:331–347.
- Heras, B., et al. 2009. DSB proteins and bacterial pathogenicity. *Nat. Rev. Microbiol.* **7**:215–225.
- Johne, B., et al. 1997. Functional and clinical aspects of the myelomonocyte protein calprotectin. *Mol. Pathol.* **50**:113–123.
- Juncker, A. S., et al. 2003. Prediction of lipoprotein signal peptides in Gram-negative bacteria. *Protein Sci.* **12**:1652–1662.
- Kall, L., A. Krogh, and E. L. Sonnhammer. 2007. Advantages of combined transmembrane topology and signal peptide prediction—the Phobius web server. *Nucleic Acids Res.* **35**:W429–W432.
- Kammer, M., C. Schon, and K. Hantke. 1993. Characterization of the ferrous iron uptake system of *Escherichia coli*. *J. Bacteriol.* **175**:6212–6219.
- Lazizzera, B. A., H. Beinert, N. Khoroshilova, M. C. Kennedy, and P. J. Kiley. 1996. DNA binding and dimerization of the Fe-S-containing FNR protein from *Escherichia coli* are regulated by oxygen. *J. Biol. Chem.* **271**:2762–2768.
- Lewis, D. A., et al. 1999. Identification of the *znuA*-encoded periplasmic zinc transport protein of *Haemophilus ducreyi*. *Infect. Immun.* **67**:5060–5068.
- Liu, J., A. J. Stemmler, J. Fatima, and B. Mitra. 2005. Metal-binding characteristics of the amino-terminal domain of ZntA: binding of lead is different compared to cadmium and zinc. *Biochemistry* **44**:5159–5167.
- Liuzzi, J. P., et al. 2005. Interleukin-6 regulates the zinc transporter Zip14 in liver and contributes to the hypozincemia of the acute-phase response. *Proc. Natl. Acad. Sci. U. S. A.* **102**:6843–6848.
- Lu, D., B. Boyd, and C. A. Lingwood. 1997. Identification of the key protein for zinc uptake in *Haemophilus influenzae*. *J. Biol. Chem.* **272**:29033–29038.
- Marchler-Bauer, A., et al. 2011. CDD: a Conserved Domain Database for the functional annotation of proteins. *Nucleic Acids Res.* **39**:D225–D229.
- Melville, S. B., and R. P. Gunsalus. 1996. Isolation of an oxygen-sensitive FNR protein of *Escherichia coli*: interaction at activator and repressor sites of FNR-controlled genes. *Proc. Natl. Acad. Sci. U. S. A.* **93**:1226–1231.
- Miller, J. H. 1972. *Experiments in molecular genetics*. Cold Spring Harbor Laboratory, Cold Spring Harbor, NY.
- Moller, L. V., et al. 1995. Multiple *Haemophilus influenzae* strains and strain variants coexist in the respiratory tract of patients with cystic fibrosis. *J. Infect. Dis.* **172**:1388–1392.
- Morton, D. J., et al. 2005. The heme-binding lipoprotein (HbpA) of *Haemophilus influenzae*: role in heme utilization. *FEMS Microbiol. Lett.* **253**:193–199.
- Morton, D. J., et al. 2007. The haem-haemopexin utilization gene cluster (*hxaCBA*) as a virulence factor of *Haemophilus influenzae*. *Microbiology* **153**:215–224.
- Moxon, E. R., and T. F. Murphy. 2000. *Haemophilus influenzae*, p. 2369–2378. In G. L. Mandell, J. R. Bennett, and R. Dolin (ed.), *Mandell, Douglas,*

- and Bennett's principles and practices of infectious diseases, 5th ed., vol. 2. Churchill Livingstone, New York, NY.
47. **Murphy, T. F.** 2003. Respiratory infections caused by non-typeable *Haemophilus influenzae*. *Curr. Opin. Infect. Dis.* **16**:129–134.
 48. **Murphy, T. F., A. L. Brauer, A. T. Schiffmacher, and S. Sethi.** 2004. Persistent colonization by *Haemophilus influenzae* in chronic obstructive pulmonary disease. *Am. J. Respir. Crit. Care Med.* **170**:266–272.
 49. **Murphy, T. F., and S. Sethi.** 2002. Chronic obstructive pulmonary disease: role of bacteria and guide to antibacterial selection in the older patient. *Drugs Aging* **19**:761–775.
 50. **Nakamoto, H., and J. C. Bardwell.** 2004. Catalysis of disulfide bond formation and isomerization in the *Escherichia coli* periplasm. *Biochim. Biophys. Acta* **1694**:111–119.
 51. **Pang, B., et al.** 2008. Lipooligosaccharides containing phosphorylcholine delay pulmonary clearance of nontypeable *Haemophilus influenzae*. *Infect. Immun.* **76**:2037–2043.
 52. **Patzer, S. I., and K. Hantke.** 2000. The zinc-responsive regulator Zur and its control of the *znu* gene cluster encoding the ZnuABC zinc uptake system in *Escherichia coli*. *J. Biol. Chem.* **275**:24321–24332.
 53. **Patzer, S. I., and K. Hantke.** 1998. The ZnuABC high-affinity zinc uptake system and its regulator Zur in *Escherichia coli*. *Mol. Microbiol.* **28**:1199–1210.
 54. **Petrarca, P., S. Ammendola, P. Pasquali, and A. Battistoni.** 2010. The Zur-regulated ZinT protein is an auxiliary component of the high-affinity ZnuABC zinc transporter that facilitates metal recruitment during severe zinc shortage. *J. Bacteriol.* **192**:1553–1564.
 55. **Raquil, M. A., N. Anceriz, P. Rouleau, and P. A. Tessier.** 2008. Blockade of antimicrobial proteins S100A8 and S100A9 inhibits phagocyte migration to the alveoli in streptococcal pneumonia. *J. Immunol.* **180**:3366–3374.
 56. **Rosadini, C. V., S. M. Wong, and B. J. Akerley.** 2008. The periplasmic disulfide oxidoreductase DsbA contributes to *Haemophilus influenzae* pathogenesis. *Infect. Immun.* **76**:1498–1508.
 57. **Sabri, M., S. Houle, and C. M. Dozois.** 2009. Roles of the extraintestinal pathogenic *Escherichia coli* ZnuACB and ZupT zinc transporters during urinary tract infection. *Infect. Immun.* **77**:1155–1164.
 58. **Saiman, L.** 2004. Microbiology of early CF lung disease. *Paediatr. Respir. Rev.* **5**(Suppl. A):S367–S369.
 59. **Schaffer, H. E., and R. R. Sederoff.** 1981. Improved estimation of DNA fragment lengths from agarose gels. *Anal. Biochem.* **115**:113–122.
 60. **Sethi, S., and T. F. Murphy.** 2001. Bacterial infection in chronic obstructive pulmonary disease in 2000: a state-of-the-art review. *Clin. Microbiol. Rev.* **14**:336–363.
 61. **Singh, I. R., R. A. Crowley, and P. O. Brown.** 1997. High-resolution functional mapping of a cloned gene by genetic footprinting. *Proc. Natl. Acad. Sci. U. S. A.* **94**:1304–1309.
 62. **Sirakova, T., et al.** 1994. Role of fimbriae expressed by nontypeable *Haemophilus influenzae* in pathogenesis of and protection against otitis media and relatedness of the fimbria subunit to outer membrane protein A. *Infect. Immun.* **62**:2002–2020.
 63. **Sonnhammer, E. L., G. von Heijne, and A. Krogh.** 1998. A hidden Markov model for predicting transmembrane helices in protein sequences. *Proc. Int. Conf. Intell. Syst. Mol. Biol.* **6**:175–182.
 64. **Tidhar, A., et al.** 2009. The NlpD lipoprotein is a novel *Yersinia pestis* virulence factor essential for the development of plague. *PLoS One* **4**:e7023.
 65. **Uehara, T., K. R. Parzych, T. Dinh, and T. G. Bernhardt.** 2010. Daughter cell separation is controlled by cytokinetic ring-activated cell wall hydrolysis. *EMBO J.* **29**:1412–1422.
 66. **van den Berg, S., P. A. Lofdahl, T. Hard, and H. Berglund.** 2006. Improved solubility of TEV protease by directed evolution. *J. Biotechnol.* **121**:291–298.
 67. **VanZile, M. L., N. J. Cosper, R. A. Scott, and D. P. Giedroc.** 2000. The zinc metalloregulatory protein *Synechococcus* PCC7942 SmtB binds a single zinc ion per monomer with high affinity in a tetrahedral coordination geometry. *Biochemistry* **39**:11818–11829.
 68. **Wahkup, G. K.** 1997. Fluorescent chemosensors for divalent zinc based on zinc finger domains. enhanced oxidative stability, metal binding affinity, and structural and functional characterization. *J. Am. Chem. Soc.* **119**:3443–3450.
 69. **Wong, S. M., and B. J. Akerley.** 2005. Environmental and genetic regulation of the phosphorylcholine epitope of *Haemophilus influenzae* lipooligosaccharide. *Mol. Microbiol.* **55**:724–738.
 70. **Wong, S. M., and B. J. Akerley.** 2003. Inducible expression system and marker-linked mutagenesis approach for functional genomics of *Haemophilus influenzae*. *Gene* **316**:177–186.
 71. **Wong, S. M., K. R. Alugupalli, S. Ram, and B. J. Akerley.** 2007. The ArcA regulon and oxidative stress resistance in *Haemophilus influenzae*. *Mol. Microbiol.* **64**:1375–1390.
 72. **Wong, S. M. S., F. St. Michael, A. Cox, S. Ram, and B. J. Akerley.** 2011. ArcA-regulated glycosyltransferase Lic2B promotes complement evasion and pathogenesis of nontypeable *Haemophilus influenzae*. *Infect. Immun.* **79**:1971–1983.
 73. **Wu, L. F., et al.** 1989. Nickel deficiency gives rise to the defective hydrogenase phenotype of *hydC* and *fur* mutants in *Escherichia coli*. *Mol. Microbiol.* **3**:1709–1718.
 74. **Wyckoff, E. E., M. L. Boulette, and S. M. Payne.** 2009. Genetics and environmental regulation of *Shigella* iron transport systems. *Biometals* **22**:43–51.
 75. **Yang, X., T. Becker, N. Walters, and D. W. Pascual.** 2006. Deletion of *znuA* virulence factor attenuates *Brucella abortus* and confers protection against wild-type challenge. *Infect. Immun.* **74**:3874–3879.
 76. **Zapun, A., and T. E. Creighton.** 1994. Effects of DsbA on the disulfide folding of bovine pancreatic trypsin inhibitor and alpha-lactalbumin. *Biochemistry* **33**:5202–5211.

Editor: J. B. Bliska